J. M. Nóbrega[1], O. S. Carneiro[1], F. T. Pinho[2], P. J. Oliveira[3]*

[1] *Institute for Polymers and Composites, Department of Polymer Engineering, University of Minho, Guimarães, Portugal*
[2] *Centro de Estudos de Fenómenos de Transporte, DEMEGI, Faculdade de Engenharia da Universidade do Porto, Porto, Portugal*
[3] *Departamento de Engenharia Electromecânica, Universidade da Beira Interior, Covilhã, Portugal*

Flow Balancing in Extrusion Dies for Thermoplastic Profiles

Part III: Experimental Assessment

A computer code, previously developed by the authors for the automatic die design, is used to optimise the flow distribution in a profile extrusion die using two alternative strategies: one based on length optimisation and the other on thickness optimisation. The numerical predictions are then compared with experimental data gathered during extrusion experiments. The numerical predictions and the experimental results agree within the experimental uncertainty thus showing the effectiveness of the computer code, the optimisation algorithm and the design strategies implemented. Generally speaking, measured and predicted values of pressure drop and flow rate are in good agreement (within 8 % and 6 %, respectively). It also is confirmed that optimisation based on thickness control leads to final profiles that are more prone to distortion.

1 Introduction

There are two main issues to solve when designing a profile extrusion die: how to make the flow distribution more uniform and how to anticipate post-extrusion effects. Of these, the former is considered to be the most influential on die performance [1 to 4]. Due to the large amount of variables involved and to the geometrical complexity of a typical extrusion die, especially in the case of complex cross-section geometries with different local flow restrictions, the design of these tools is usually based on trial-and-error procedures, which may be exclusively empirical, or result from a combination of experimental and computational work. Even in the latter case, and in spite of the use of numerical aids, the task is very time consuming and relies essentially on the designer's experience, since the decisions necessarily involved in this process are always committed to the designer [3].

The design of profile extrusion dies has been the subject of investigation for quite a long time [5], and there are various works in the literature that report the accumulated experience and suggest practical rules for improved design of these tools [5 to 10]. In some cases, these recommendations combine empirical rules with analytical calculations to provide the designer with a better insight of the phenomena involved [6, 7, 11].

The progressive development of computational fluid dynamics and the availability of accurate numerical codes have allowed die designers to use the computer as a powerful design aid. In fact, nowadays it is possible to model accurately the flow of molten polymers in extrusion dies using three-dimensional modelling codes, and it is fair to recognize that most of them are based on the finite element method [12 to 14]. However, the associated calculation times are often prohibitive and demand heavy computational resources. These requirements are particularly critical when optimisation algorithms are used, since the searching process requires the solution of several fluid dynamic trials to arrive at the final solution. As a consequence, three-dimensional numerical calculations have so far been used only to solve some specific problems [15 to 17] and general design techniques, such as the network based flow analysis [18 to 20] and the cross section methods [16, 21], are always a compromise between accuracy and swiftness of calculations [22, 23]. Anyway, 3D computations are generally mandatory to capture adequately all the flow details [16, 23, 24], especially for complex geometries.

In terms of the techniques used to optimise the flow channel of profile extrusion dies there are two main approaches: some authors claim that this should be done through changes in the flow channel parallel zone cross-section [1, 5, 22] (or die land) whereas others argue that the parallel zone cross-section should be kept untouched and all modifications of the flow channel should be done in the upstream regions [21, 25, 26]. Some works have shown that the optimisation techniques based on adjustments of the parallel zone cross-section generate more robust dies, i. e., leading to flows less sensible to variations in process conditions and/or material rheology [1, 27]; however, if the profile dimensions are an issue, this approach increases the propensity of the profile to distortion, since it promotes the occurrence of different draw-down ratios [27]. The latter design approach, in contrast, minimizes differential pulling, but it may be insufficient to entirely balance geometries with

* Mail address: O. Carneiro, Department of Polymer Engineering, Universidade do Minho, 4800-058 Guimarães, Portugal
E-mail: olgasc@dep.uminho.pt

IPP_ipp_2004_03_1825 – 22.6.04/druckhaus

several different flow restrictions [27]. The use of flow separators may help to solve this problem [26, 27], but makes the die more sensitive to process variations [27] and gives rise to the formation of weld lines, which may negatively affect the mechanical performance of the extruded profile.

It was the need for a design process less dependent on personal knowledge that motivated the development of the automatic die design concept [3, 28 to 32]. This is also the main purpose of a die design code currently under development, whose main objective is the automatic search of the optimal flow channel geometry. The code includes an optimisation routine, which is coupled with geometry and mesh generators, as well as routines for fluid flow and heat transfer calculation.

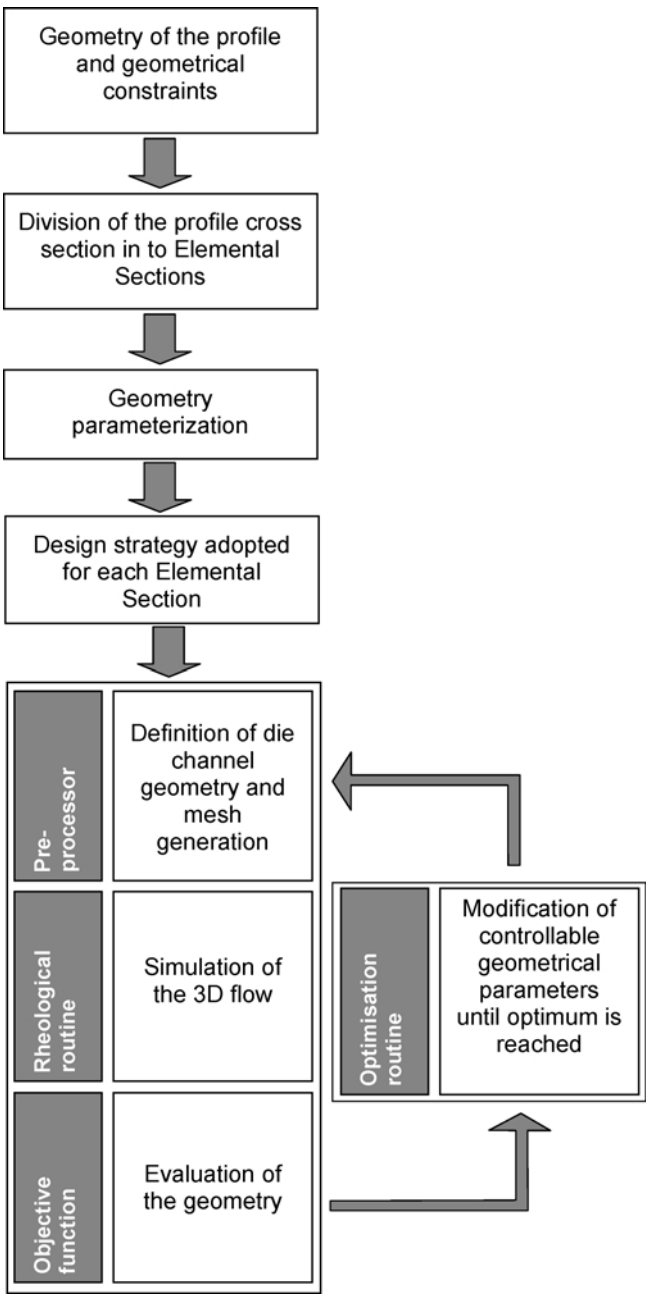

Fig. 1. Optimisation methodology

The calculation procedure is based on the finite volume methodology and is able to predict, within acceptable computation times, the complex 3D flow patterns that are formed, and the corresponding local fluid temperature variations due to viscous heat dissipation and/or specific thermal boundary conditions [28].

In this work, our die design code is used to optimise the flow channel of a specific profile extrusion die, and the corresponding numerical results are compared with experimental data, gathered during extrusion experiments performed with the same dies, for the purpose of validation. In particular, this set of experiments enabled us to assess the predictive capacity of the computational rheology code and the effectiveness of the optimisation algorithm and design strategies implemented.

The first part of the work (section 2) briefly presents the methodology and the code developed to automatically balance the flow in profile extrusion dies. The design and optimisation of the flow channel as well as the experimental procedure, are described in section 3. The experimental results are presented and discussed in section 4 and, finally, the conclusions are drawn in section 5.

2 Die Design Code

The code developed by *Nóbrega* et al. [28] designs the flow channel of extrusion dies according to the sequence of operations schematically represented in Fig. 1. It starts with the profile geometry definition, followed by the division of the flow channel cross-section into elemental sections (ES) and the subsequent parameterization of the flow channel geometry. Following the methodology proposed in [28] the flow channel is initially divided into four main zones (see Fig. 2A): adapter (A), transition zone (TZ), pre-parallel zone (PPZ) and parallel zone (PZ). Since PPZ has a similar shape to PZ, but is thicker, it is possible to parameterize the geometry with the following quantities: distance to the die exit, or length of constant thickness, (L), angle of convergence (θ), PPZ thickness (t2) and PZ thickness (t1) (see Fig. 2A).

In the next step, the design strategy to control the flow in each ES (shown in Fig. 2B) must be selected. Bearing in mind that some of the flow channel parameters have a minor influence on the flow distribution [29] and assuming that the dimensions of the profile to be produced are highly restricted, two main strategies are recommended for this task [27, 28]: one is based on the control of the length (L) and the other is based on the control of thickness (t1). When the length (L) is the controllable parameter, the PZ cross section is kept constant and the polymer melt is expected to emerge from the die flow channel at a similar average velocity in all ES; consequently, the draw-down ratio will be almost constant throughout the whole profile cross-section. On the other hand, when the thickness is the controllable parameter, the PZ cross-section is modified. In this case, to obtain the prescribed profile thickness the melt must emerge from the die lips at different velocities; therefore, the ES are subjected to different draw-down ratios. A study of the performance and sensitivity of dies optimised with these two different strategies (here referred to as DieL and DieT, respectively) can be found in *Carneiro* et al. [27].

IPP_ipp_2004_03_1825 – 22.6.04/druckhaus

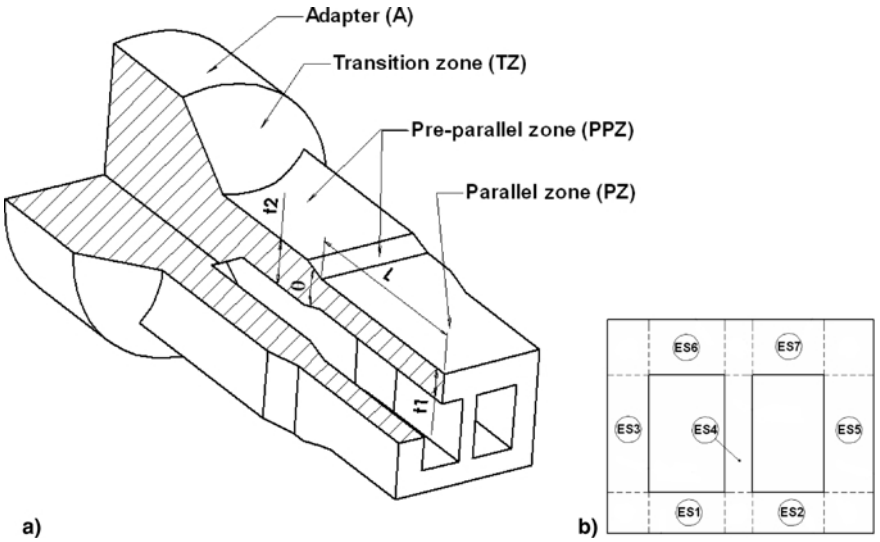

Fig. 2. Flow channel of a profile extrusion die A: identification of its main zones, B: geometrical controllable parameters considered in the definition of the PPZ

The optimisation routines, whose purpose is to find the set of geometrical parameters that better approach the required flow distribution, are initialised with the specification of trial values for these parameters so that an initial (trial) geometry can be generated. For the flow simulation, a three-dimensional computational mesh needs to be deployed over that geometry. In order to minimise the time spent on the calculations, which is proportional to the number of points in the mesh, coarse meshes are employed at the initial general iterations of the optimisation code, being progressively refined as the final solution is approached. Since the flow distribution is dominated by the most restrictive zones, PPZ and PZ [3, 4, 28, 29], during the optimisation process it suffices to model the flow in these die zones.

The 3D flow and temperature fields are calculated with a computational code based on the finite volume method, comprising a set of routines to model each relevant physical process. This code has been developed by the authors [33, 34] and has recently been extended to deal with non-isothermal flows [35]. The results of the simulations are used to evaluate the global performance of each trial geometry by resorting to an objective function (F_{obj}), described elsewhere [28], where the individual contribution of each ES is considered. This combines two criteria – flow balance and ratio L/t (length/thickness) – affected by different weights. Here it suffices to mention that the objective function is always positive and is defined in such a way that its value decreases with increasing performance of the die, being zero for a perfectly balanced condition with all the ES lengths in the advisable range.

The final step of the whole design process consists on the iterative geometry correction. For this purpose, two algorithms were implemented: one is based on the SIMPLEX method and the heuristic of the other mimics the experimental trial-and-error procedure usually employed to manufacture extrusion dies (see [28] for details). The "final" geometry is attained when, at the prescribed highest mesh refinement stage (usually with 10 computational cells across the thickness of the walls), the algorithm is unable to further improve the geometry performance.

3 Case Study

The parallel zone cross section of the extrusion die to be optimised is shown in Fig. 3. It is composed by several subsections of different thickness, ranging from 2 to 4 mm, all other dimensions being presented in Table 1. These values were imposed deliberately in order to promote different local flow restrictions, a realistic situation that may represent typical profile extrusion dies.

The polymer used in this work was a polypropylene homopolymer extrusion grade, Novolen PPH 2150, from Targor. Its rheological behaviour was characterised experimentally in ca-

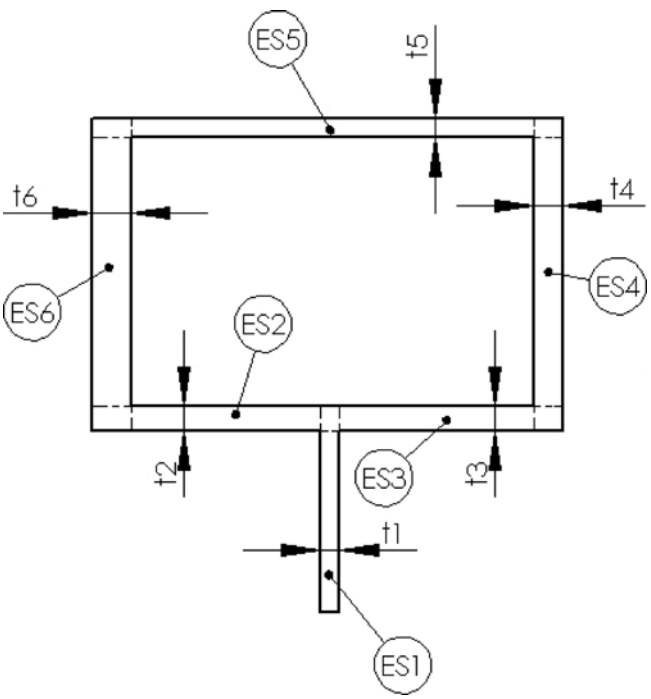

Fig. 3. Cross section of the parallel zone (PZ) of the die used as a case study, subdivision in elemental (ES) sections and identification of the optimisation parameters related to thickness

IPP_ipp_2004_03_1825 – 22.6.04/druckhaus

ES	1	2	3	4	5	6
t_i mm	2.0	2.5	2.5	3.0	2.0	4.0
L_i mm	30.0	37.5	37.5	45.0	30.0	60.0
L_i/t_i	15.0	15.0	15.0	15.0	15.0	15.0

Table 1. Initial flow channel dimensions

pillary and rotational rheometers, and the shear viscosity data was fitted with a least-squares method by means of the Bird-Carreau constitutive equation combined with the Arrhenius law, as described in [28].

In the remaining of this section, we describe the numerical optimisation procedure for the case study under consideration and give some details of the experiments used to acquire data for validation.

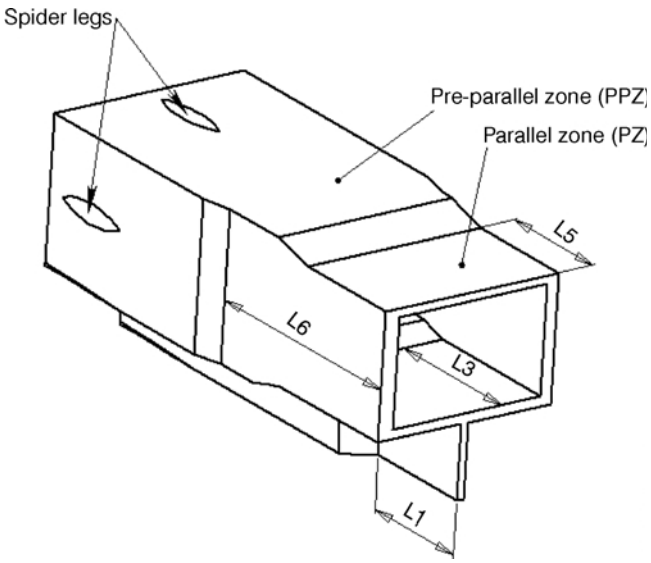

Fig. 4. Die flow channel used as a case study: region corresponding to parallel and pre-parallel zones (PZ + PPZ), identification of some of the optimisation parameters related to length and location of the spider legs

Flow rate* kg/h	20
Melt inlet temperature °C	230
Outer die walls temperature °C	230
Inner (mandrel) die walls	Adiabatic

* Corresponding to an average velocity of 1 m/min at the die exit

Table 2. Operating and thermal boundary conditions used in the flow simulations

3.1 Numerical Optimisation

For the purpose of optimisation, the flow channel cross section was divided into 6 elemental sections (ES), as shown in Fig. 3, and the initial (trial) geometry adopted for the flow channel (PPZ + PZ) is depicted in Fig. 4, where the location of the spider legs needed to hold the inner die mandrel is also shown.

This flow channel geometry was then optimised using the two control approaches described in detail in *Nóbrega* et al. [28] and briefly outlined in sections 1 and 2. The control strategy based on the length optimisation resulted in a geometry denoted DieL, whereas the strategy based on the thickness optimisation resulted in geometry DieT. In both cases, the experimental-based optimisation algorithm of [28] was applied using 5 variables denoted as: Opt1 for ES1, Opt2–3 for ES2 and ES3, Opt4 for ES4, Opt5 for ES5 and Opt6 for ES6. These variables assume the value of either the ES length, or the ES thickness, for the optimisation of DieL and DieT, respectively. In order to facilitate the subsequent die machining, ES2 and ES3 were set equal; consequently, only one variable was used for these two ES.

For the first trial of the optimisation algorithm, a constant L/t equal to 15 was adopted for all ES (see Table 1); the operating and thermal boundary conditions prescribed for the flow simulations are listed in Table 2.

As mentioned above, the optimisation algorithm initially calculates the flow of the polymer melt using a coarse mesh which is then progressively refined as the procedure evolves towards a final solution. The initial meshes were rather coarse, with 2 cells along the thickness for each ES mapped; in this case, a typical mesh is composed by 7500 computational inner

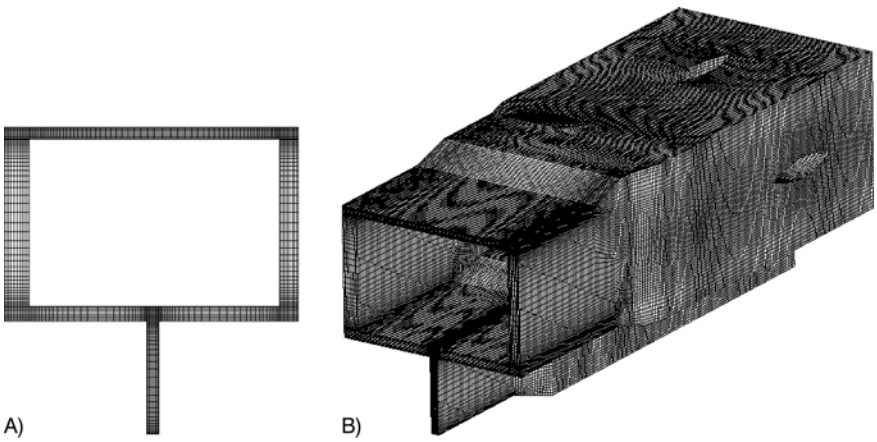

Fig. 5. Typical mesh used in the calculations, at the highest mesh refinement stage
A: cross section of the parallel zone; B: global 3D view

IPP_ipp_2004_03_1825 – 22.6.04/druckhaus

cells and the number of degrees of freedom is approximately 37 500. The most refined meshes, used during the final stages of the calculation process, had 10 cells across the thickness for each ES, as shown in Fig. 5, which implies 570 000 computational cells and 2 850 000 degrees of freedom. The calculation time required for the grid generation and the flow field computation was approximately 36 s and 7 h for the coarsest and the finest meshes used, respectively, on a Pentium IV computer running at 2.4 GHz.

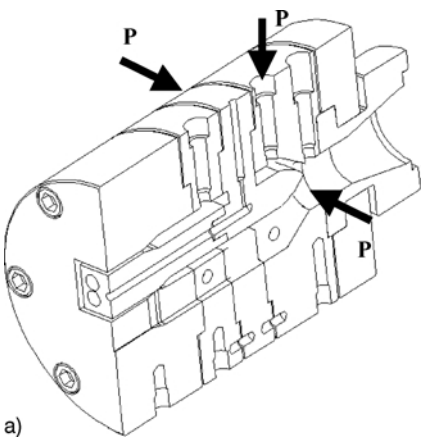

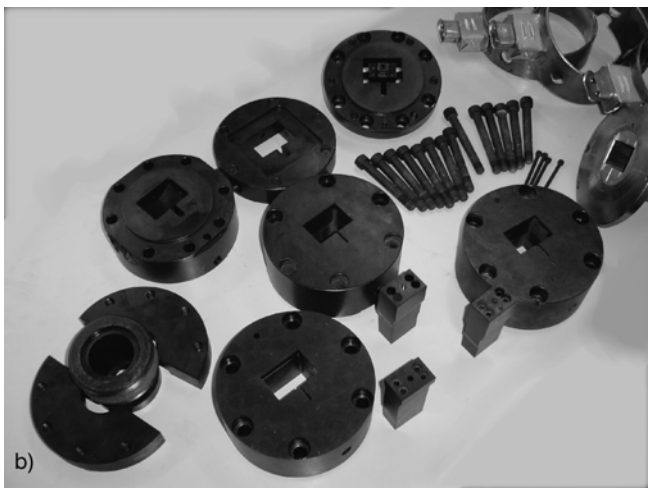

Fig. 6. Modular extrusion dies used in the experimental work A: sectioned view of a typical die and location of the pressure transducers (P), B: set of pieces used to built all the dies

Run ID	Extrusion die	Mass flow rate kg/h	Die wall temperature °C	Average melt exit velocity m/min
INI	DieINI	20.4	230	0.99
L1	DieL	19.8	230	0.96
L2	DieL	19.7	250	0.95
L3	DieL	13.8	230	0.67
T	DieT	19.3	230	0.90

Table 3. Extrusion experiments performed

3.2 Experimental Facility and Techniques

To assess and validate the results of the simulations we carried out the following experiments. Three modular instrumented extrusion dies were designed and manufactured: one using the same L/t ratio for all elemental sections (DieINI) and matching the initial trial of the optimisation algorithm, and the other two dies (DieL and DieT) corresponding to the optimised geometries proposed by the die design code.

The constructive solution adopted for the dies is shown in Fig. 6. Their modular conception enables us to built the die flow channel (corresponding to DieINI, DieL or DieT) changing only the last die region (mandrel and outer part), since the remaining components are common to all geometries. In order to monitor the process, the extrusion dies were instrumented with several pressure transducers located at the beginning of the PPZ ("P" in Fig. 6A), from Terwin, model 2000 series, that have an accuracy of 0.5 % FSD. Considering the measured pressures and the propagation of uncertainties we estimate the total uncertainty to vary between 8 % and 10 % for the highest and lowest pressures, respectively.

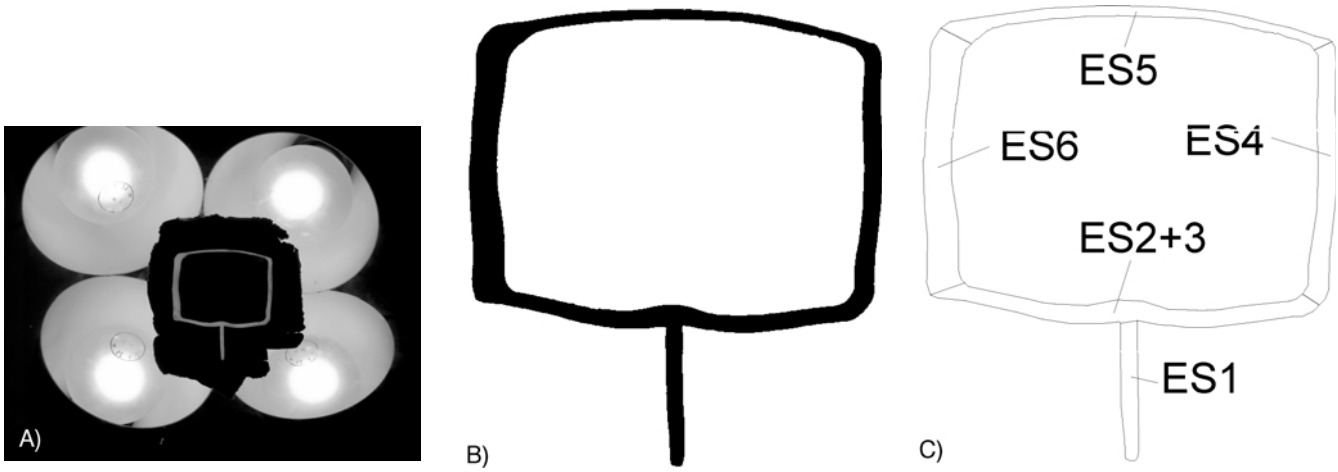

Fig. 7. Methodology adopted to measure the areas of the extruded profiles

IPP_ipp_2004_03_1825 – 22.6.04/druckhaus

Extrusion experiments were carried out in a single-screw extruder (screw diameter of 45 mm and L/D = 20) using the polypropylene extrusion grade under different operating conditions. The set of runs performed is described in Table 3 and includes similar conditions to those used during the design stage. Since DieL (based on length optimisation) is expected to be the most sensitive to processing conditions [1, 2, 27], different throughputs and die temperatures were tested. For assessment purposes, all the experimental runs were simulated with the computer code.

To assess the flow distribution it is necessary to quantify the flow rate in each ES at the die exit. The direct measurement of local flow rates in polymer extrusion is extremely difficult [3], hence they have to be estimated from the cross section area. Assuming that after leaving the die flow channel the melt does not migrate among ES, neglecting differences in shrinkage between thicker and thinner sections, and since all sections are pulled simultaneously by the haul-off unit at the same velocity, the relative flow distribution can be evaluated through the measurement of the relative area of each ES, as suggested by *Szarvasy* et al. [3]. The protocol used to measure the profile ES areas, which are shown in Fig. 7, was the following:

1. Slices of the profile were cut at different axial locations;
2. Each slice was surrounded by plasticine and photographed with a digital camera using a back illumination setup – Fig. 7A. As the material is translucent, the profile area can be easily identified. The digital photo was sent to a computer and was automatically processed using a commercial image editor. After this step a new image was created (see Fig. 7B);
3. The new image was vectorized and the profile elemental areas (identified in Fig. 7C) were measured using a commercial CAD software.

To eliminate difficulties in identifying the ES limits, the corner zones were included in the measurements and divided by the two adjacent ES, and the areas corresponding to ES2 and ES3 were merged.

There are two main sources of uncertainty in measuring the area of each ES: the inherent variation of cross section dimensions of the ES along the extrudate, which leads to the precision uncertainty, and the ± 1 pixel systematic uncertainty in measuring the corresponding ES thickness.

The total relative uncertainty (U_M/M) in the measured relative area M of each ES is given by Eq. 1:

$$\frac{U_M}{M} = \sqrt{\left(\frac{1}{N_P}\right)^2 + \left(\frac{t\sigma}{M\sqrt{N}}\right)^2}, \qquad (1)$$

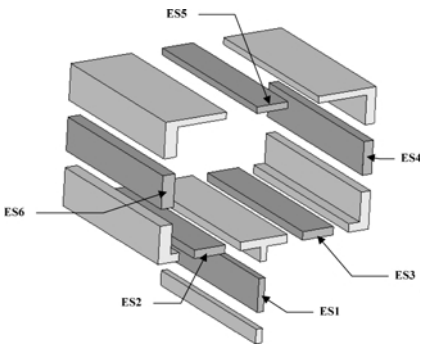

Fig. 8. Location of the samples used in the annealing tests

where N_P is the number of pixels across the thickness, M is the average value of the sample measured relative cross section area, σ is the sample standard deviation, N is the sample size and t is the t-distribution parameter at a 95 % confidence level.

To evaluate the level of induced internal stresses, a longitudinal sample of each ES was cut as described in Fig. 8. Each sample was annealed in an oven at 170 °C for 15 min and then their lengths were measured.

The results of all these measurements are presented in the next section and compared with the results of the numerical predictions.

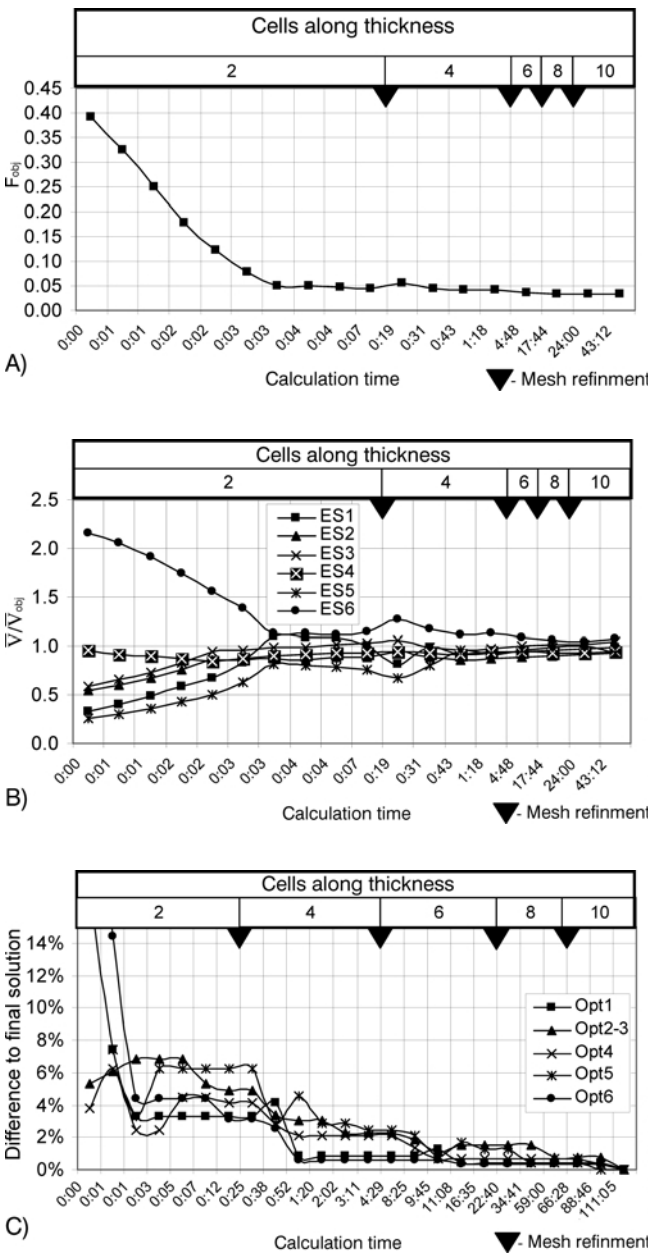

Fig. 9. Results of simulations performed during the optimisation process of the DieL
A: objective function, B: ratio between the actual velocity and the objective velocity for each elemental section (V/V_{obj}), C: difference between the actual value of the optimisation variable and the corresponding final optimised value

IPP_ipp_2004_03_1825 – 22.6.04/druckhaus

4 Results and Discussion

The results of the numerical simulations are presented first and are followed by their comparison with the experimental data.

Results of the optimisation of DieL and DieT in terms of the predicted values of the objective function value (F_{obj}), velocity ratio $\bar{V}/\bar{V}_{obj}$ (ratio between actual and required average velocities, for each ES) and relative difference between actual and final values of each optimisation variable, are plotted in Figs. 9 and 10, respectively. It is clear that the initial trial geometry is highly unbalanced, with the velocities in ES1 (the most restrictive section) and ES6 (the least restrictive section) differing from 30 % and 200 % from the required values, respectively, thus leading to an initial value of F_{obj} of approximately 0.4. The optimisation routines substantially improved the flow distribution, as quantified both by the low final value of F_{obj} (0.03 for DieL and 0.01 for DieT) and by the final values of the ratio $\bar{V}/\bar{V}_{obj}$, all close to 1.0. In spite of the relatively large computational time required for the complete optimisation process (43 h for DieL and 111 h for DieT), it is noted that after approximately 4 hours of calculation all the optimisation variables differ from their final values by less than 5 %, in both cases (see Figs. 9C and 10C). Additionally, it is important to note that the design process was completely automatic, i. e., the optimisation was fully controlled by the computer without any user intervention.

The evolution of the flow distribution along the optimisation process can also be observed in the contour plots of $\bar{V}/\bar{V}_{obj}$, shown in Fig. 11, corresponding to some steps of the process. This improvement is also confirmed by the decrease of the ratio between the maximum of all bulk ES velocities and each bulk ES velocity, $\bar{V}_{max}/\bar{V}$, between the initial trial (DieINI) and the optimised (DieL and DieT) dies, shown in Table 4. The maximum values of this ratio were reduced from 7.46, at the initial trial geometry, to 1.15 and 1.68 for DieL and DieT, respectively.

As explained in section 3.1, both Fig. 11 and Table 5, where the final dimensions of the optimised dies are given,

Extrusion die	ES1	ES2	ES3	ES4	ES5	ES6
DieINI	6.20	3.72	3.39	2.18	7.46	1.00
DieL	1.08	1.15	1.03	1.12	1.15	1.00
DieT	1.68	1.38	1.33	1.24	1.56	1.00

Table 4. Ratio V_{max}/V obtained numerically for the initial trial and optimised extrusion dies

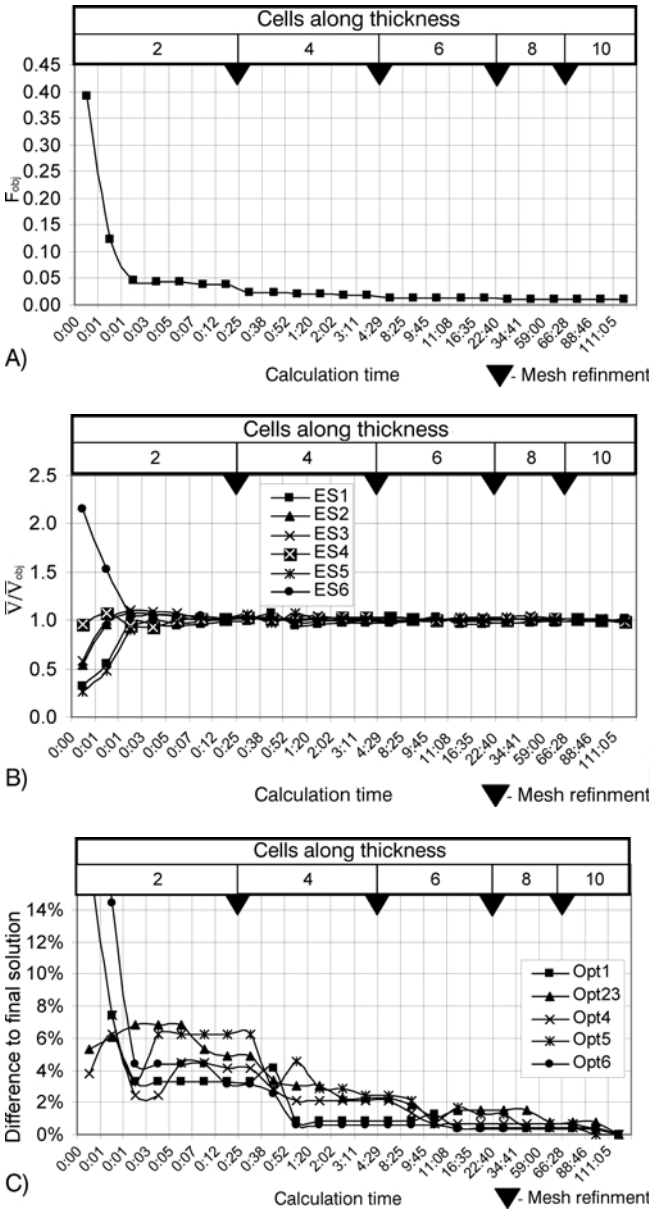

Fig. 10. Results of simulations performed during the optimisation process of the DieT
A: objective function, B: ratio between the actual velocity and the objective velocity for each elemental section (V/V_{obj}), C: difference between the actual value of the optimisation variable and the corresponding final optimised value

		ES1	ES2	ES3	ES4	ES5	ES6
DieL	t_i mm	2.0	2.5	2.5	3.0	2.0	4.0
	L_i mm	7.50	11.50	11.50	17.50	7.00	60.00
	L_i/t_i	3.75	4.60	4.60	3.83	3.5	15.0
DieT	t_i mm	2.42	2.64	2.64	2.89	2.42	3.19
	L_i mm	30.0	37.5	37.5	45.0	30.0	60.0
	L_i/t_i	12.40	14.20	14.20	15.57	12.40	18.81

Table 5. Optimised flow channel dimensions

IPP_ipp_2004_03_1825 – 22.6.04/druckhaus

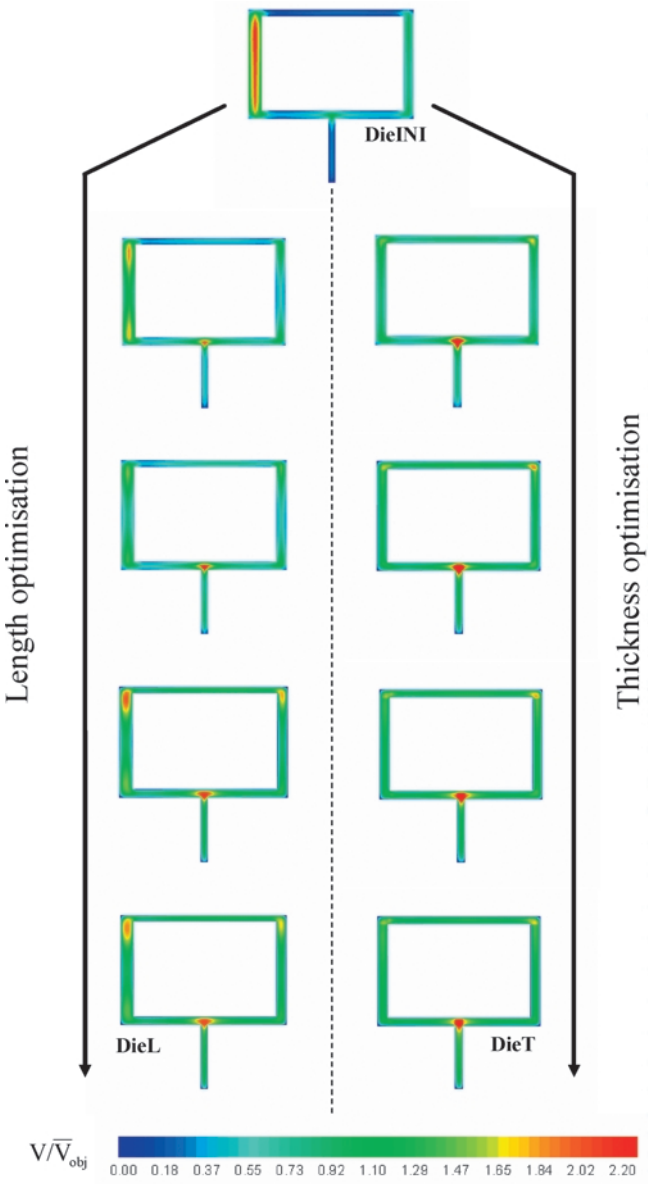

Fig. 11. Contours of the ratio $V/\bar{V}_{obj}$ corresponding to some steps of the optimisation procedure

show that the optimisation of DieL does not involve any change in the die land cross-section, which is certainly not the case for DieT. Consequently, in DieL the extrudate leaves the extrusion die at similar velocities, while in DieT the velocities must be different, in order to obtain the required profile dimensions. This explains the higher values of $\bar{V}_{max}/\bar{V}$ for DieT seen in Table 4.

As expected, the data in Table 5 for DieL show a drastic reduction in the final L/t ratios for all ES except ES6, which have the thickest wall. In contrast, for DieT the values of L/t are larger. As noted in [1, 3] and confirmed in [27], an extrusion die with low L/t values has a naturally higher sensitivity to processing conditions because the length of its parallel zone is insufficient to filter oscillations coming from upstream regions. The differences between DieL and DieT can be further understood by analysing the flow streamlines. Fig. 12 shows calculated streamtraces in the region corresponding to ES5, one of the thinner walls, for all the manufactured dies. In all cases differences in thickness promote lateral flux, from thinner to thicker regions. Therefore, for DieL (having a shorter parallel zone but equal cross section to DieINI) the melt leaves the die channel before a fully developed flow is attained, to avoid loosing the flow balance obtained upstream. On the other hand, for DieT the flow becomes fully developed in the parallel zone and this contributes to its higher stability, typical of the dies optimised through thickness adjustment [1, 3, 27].

Fig. 13 shows photographs of the polymer melt emerging from the dies, during the experiments, and the corresponding computed velocity fields. For the initial trial die (DieINI), the excessive flow in the thicker ES produces a clearly visible melt rippling, but this was eliminated in the optimised dies. It is important to mention that as the melt is expected to emerge at different velocities from DieT, melt rippling would be a possibility here. However, the ratio between the maximum and minimum average velocities in DieT is significantly lower than in DieINI (see Table 4), and in this way melt rippling is avoided.

Table 6 compares measured and predicted pressure drops for all the extrusion runs listed in Table 3. The predicted values are always lower than the measured data, showing a maximum difference not exceeding 8.8 %, a value of the same order of magnitude of the experimental uncertainty.

Despite the good match between the measured and predicted pressure drop values, some of the trends of the results in Ta-

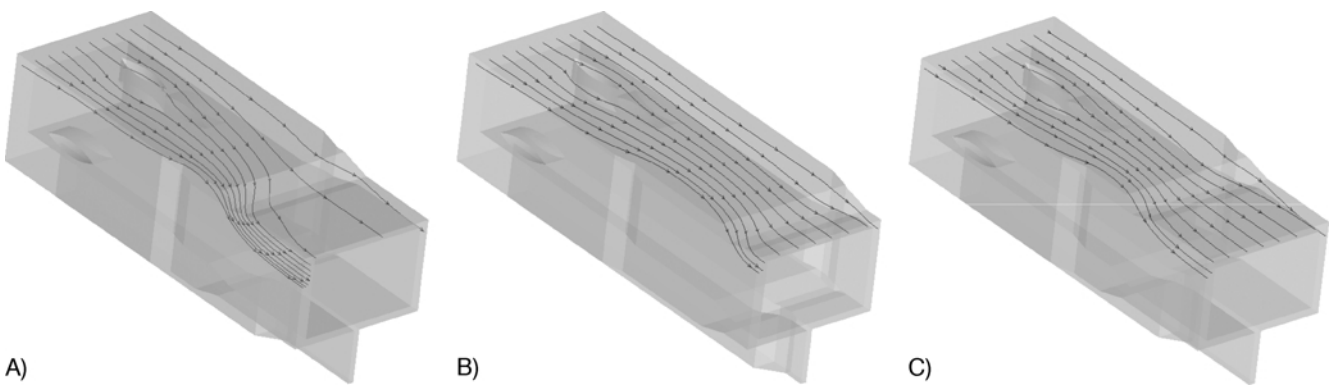

Fig. 12. Streamlines developed in ES5
A: DieINI, B: DieL, C: DieT

IPP_ipp_2004_03_1825 – 22.6.04/druckhaus

ble 6 are not intuitive as discussed now. These counter-intuitive trends are mainly due to differences in viscous dissipation (and, thus, in temperature), which is dependent on both shear rate (related to channel thickness) and residence time (related to channel length). Some of the results in Table 7 facilitate this interpretation. For example, it would be expected that DieINI would lead to higher pressures than DieT, since both have similar lengths but the former has lower ES thicknesses. However, the predicted values are similar (3.65 MPa). This is an indirect consequence of the unbalanced flow distribution occurring in

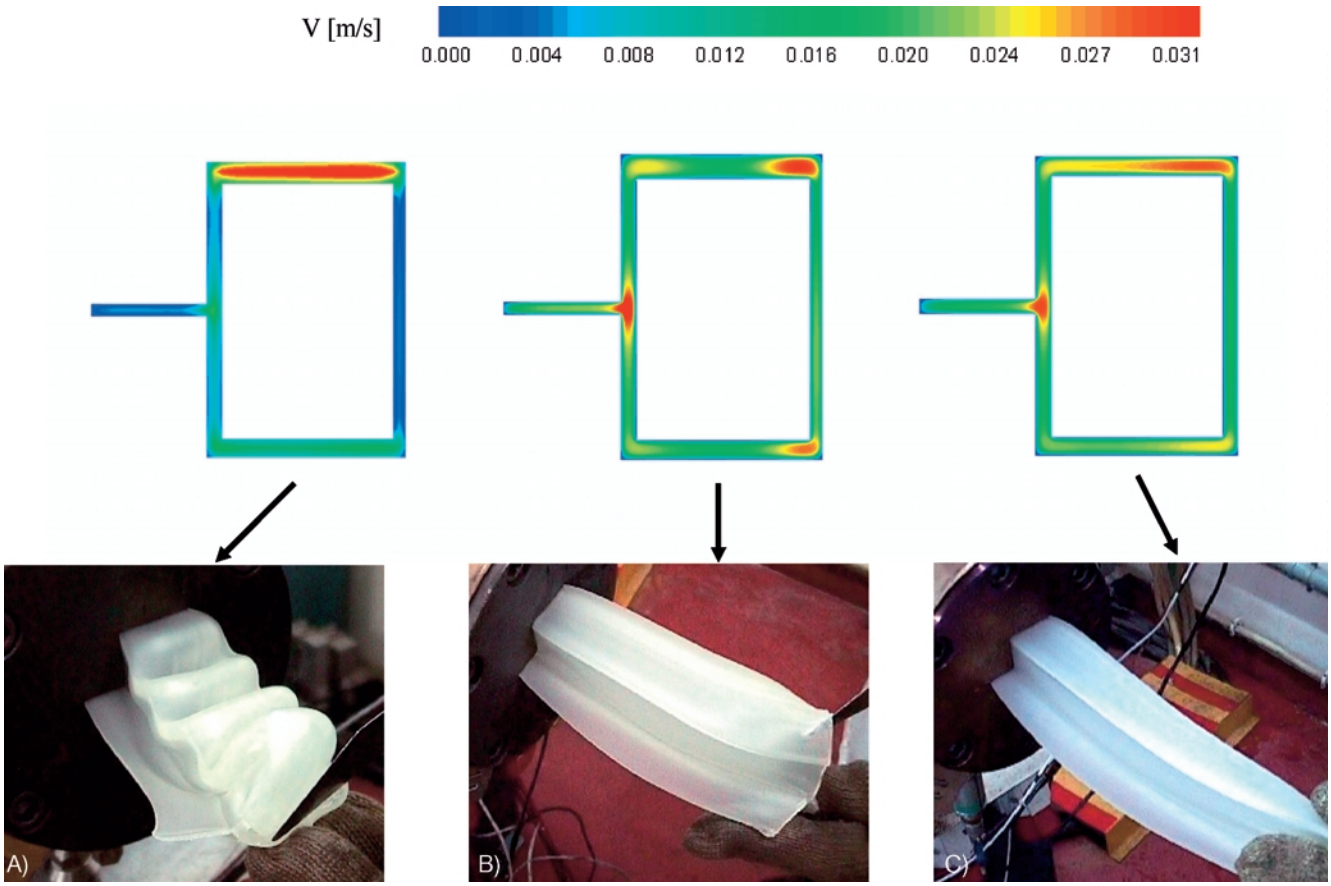

Fig. 13. Velocity contours and polymer melt leaving the die flow channel (photo taken during extrusion)
A: DieINI, B: DieL, C: DieT

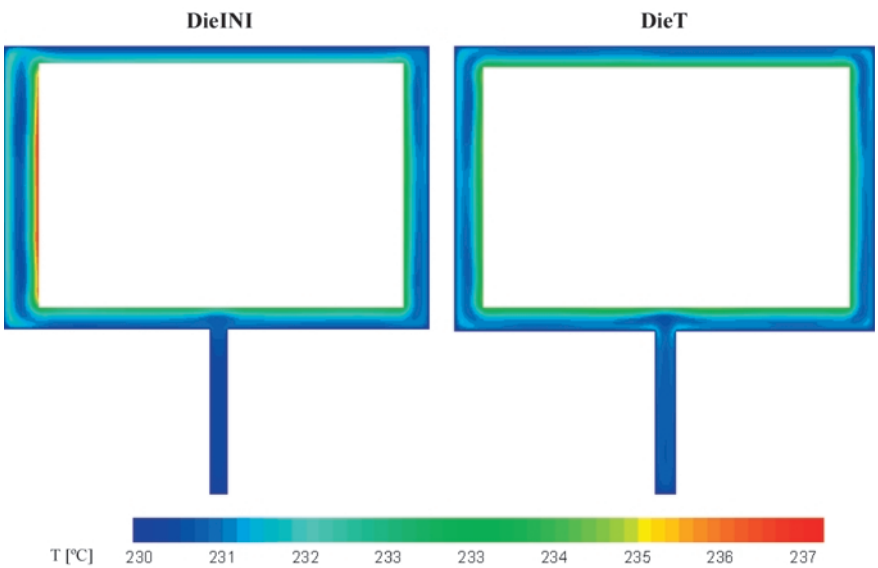

Fig. 14. Outlet temperature contours predicted for DieINI and DieT

IPP_ipp_2004_03_1825 – 22.6.04/druckhaus

DieINI (see Table 4). Since the flow is concentrated in the thicker section (ES6) in the remaining, thinner, sections it is reduced, decreasing the corresponding pressure drop. Simultaneously, the higher viscous dissipation occurring in ES6 (see Table 7), evidenced in Fig. 14, is also responsible for the decrease in the pressure drop.

Table 8 compares the predicted and the measured flow distributions. Generally speaking, the numerical predictions are in excellent agreement with the experimental measurements considering the corresponding experimental uncertainty of these difficult measurements. The maximum difference is of about 11.5 % occurring in ES2 + 3 of DieINI, but usually the differences are of the order of just a few percent.

The values of $\bar{V}_{max}/\bar{V}$ in Table 4 can be interpreted as the relative draw-down ratios at which the different ES of the profile are subjected to. Different draw-down ratios across the exit section are expected to induce different levels of residual stresses and, as a consequence, the profiles produced with DieT may

Run ID	Pressure drop		
	Predicted MPa	Measured value* MPa	Difference %
INI	3.65	4.00	−8.75
L1	2.56	2.80	−8.57
L2	2.48	2.56	−3.13
L3	2.31	2.45	−5.71
T	3.65	3.84	−4.95

* Average value of the three pressure transducers whose location is shown in Fig. 6A

Table 6. Comparison between predicted and measured pressure drop values

Run ID	Maximum shear rate 1/s	Melt temperature at the die exit °C	
		Average	Maximum
INI	135.81	231.4	237.0
L1	135.00	231.0	233.9
L2	134.39	236.6	250.1
L3	94.55	230.8	233.0
T	109.65	231.3	234.8

Table 7. Predictions of maximum shear rate, average and maximum temperature at the die exit

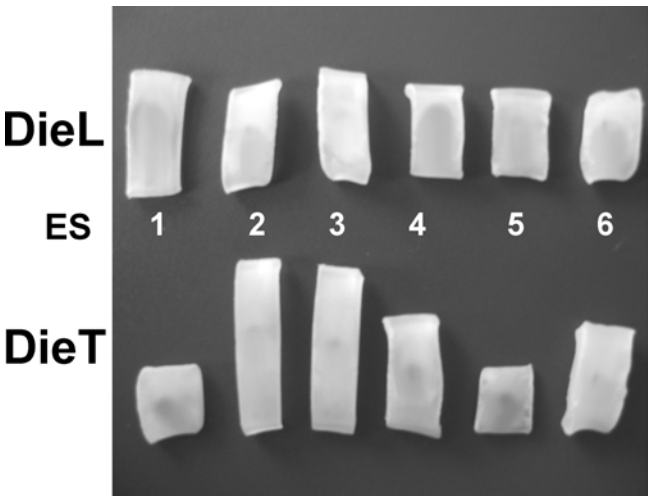

Fig. 15. Profile samples after annealing A: DieL, B: DieT

Run ID		ES1	ES2 + 3	ES4	ES5	ES6
INI	M	3.2	18.3	19.2	7.1	52.2
	P	2.9	16.2	19.2	6.7	55.0
	D	−9.4 %	−11.5 %	0.0 %	−5.6 %	5.4 %
	U	9.0 %	9.5 %	4.2 %	14.2 %	3.9 %
L1	M	8.3	26.0	18.7	18.2	28.7
	P	8.2	25.4	19.1	18.9	28.4
	D	−1.2 %	−2.3 %	2.1 %	3.8 %	−1.0 %
	U	6.7 %	4.9 %	5.6 %	8.8 %	3.9 %
L2	M	8.8	25.4	18.7	18,.2	28.7
	P	8.8	25.0	19.1	18.7	28.3
	D	0.0 %	−1.6 %	2.1 %	5.1 %	−3.1 %
	U	4.8 %	4.5 %	4.5 %	8.3 %	3.7 %
L3	M	8.0	25.5	18.7	18.5	29.4
	P	8.2	25.4	19.1	18.8	28.5
	D	2.5 %	−0.4 %	2.1 %	1.6 %	−3.1 %
	U	4.8 %	4.5 %	4.5 %	8.3 %	3.7 %
T	M	7.4	26.2	20.2	20.2	26.0
	P	7.4	25.8	19.7	20.3	26.8
	D	0.0 %	−1.5 %	−2.5 %	0.5 %	3.1 %
	U	6.3 %	4.4 %	4.9 %	8.2 %	5.6 %

Table 8. Relative elemental cross-section areas: measured areas (M), predicted areas (P), difference between predicted and measured areas (D) and overall uncertainty (U) of measured values

IPP_ipp_2004_03_1825 – 22.6.04/druckhaus

have a higher tendency to distort. This was confirmed by the results of the annealing tests shown in Fig. 15. The retraction of the samples cannot be directly correlated with the stresses induced by pulling, because there are several other phenomena involved (for example, thicker sections have a higher cooling time and, consequently, have more time to relax internal stresses). However, the ratio between the longest and the shortest sample after annealing have values of approximately 1.4 for DieL and 2.6 for DieT, an indication that DieT produces profiles with a stronger tendency to distortion.

5 Conclusion

In this work a numerical methodology, which has been developed by the authors to carry out the automatic optimisation of profile extrusion dies, is further tested and is compared with results from experiments. The design methodology was here used to optimise the flow channel of an extrusion die using two alternative approaches: variation of the length of the die elemental sections or variation of their thicknesses. In the experiments, three extrusion dies were produced and their extrudates measured. The first geometry corresponded to the initial trial die submitted to the optimisation algorithm, and the other two dies corresponded to the optimised geometries.

The main conclusions of this work are the following:

i) The optimisation algorithm improved significantly the extrusion die flow distribution thus demonstrating the effectiveness of the numerical methodology and design strategies implemented.

ii) The experimental measurements and the flow dynamic results of the numerical calculations were in excellent agreement, within the experimental uncertainty, thus demonstrating the ability of the code to predict the melt flow distribution and pressure drop for all dies/processing conditions considered. Thus, it may be asserted that the present computer code is a valuable tool to aid the design of extrusion dies.

iii) Extrusion dies optimised on the basis of length control have a higher sensitivity to processing conditions compared to those optimised on the basis of thickness.

iv) Profiles produced with dies optimised with thickness control have more tendency to distort due to the induced internal stresses.

References

1 *Svabik, J., Mikulenka, T., Manas, M., Busby, J. W.:* Paper presented at PPS Regional Meeting Europe/Africa, Gothenburg, Sweden (1997)

2 *Sienz, J., Pittman, J. F. T., Ettinger, H., Bates, S. J.:* Paper presented at the 5th ESAFORM Conference, Krakow, Poland (2002)

3 *Szarvasy, I., Sienz, J., Pitman, J. F. T., Hinton, E.:* Int. Polym. Process. 15, p. 28 (2000)

4 *Sienz, J., Bulman, S. D., Pitman, J. F. T.:* Paper presented at the 4th ESAFORM Conference, Liege, Belgium (2001)

5 *Corbett, H. O.:* SPE J., June, p. 15 (1954)

6 *Levy, S.:* Adv. Plast. Tech., January, p. 8 (1981)

7 *Levy, S.:* Adv. Plast. Tech., October, p. 24 (1981)

8 Extruded Plastics Profiles, Cranne Plastics Company, www.cranne-plastics.com (1998)

9 *Rauwendaal, C.:* Plastics World, November, p. 73 (1991)

10 *Kaplun, Ya. B., Levin, A. N.:* Soviet Plast. 1, p. ■ (1965)

11 *Michaeli, W.:* Extrusion Dies for Plastic and Rubber. Hanser, Munich, Vienna, New York (1992)

12 Polyflow software, Fluent Inc., http://www.fluent.com

13 Polycad, http://www.polydynamics.com

14 Flow2000, Compuplast, http://www.compuplast.com

15 *Rubin, Y.:* Caotchoucs & Plastiques, 773 (December), p. 39 (1998)

16 *Svabik, J., Placek, L., Saha, P.:* Int. Polym. Process. 14, p. 247 (1999)

17 *Cavka, E., Marchal, T.:* Paper presented at the 4th ESAFORM Conference, Liege, Belgium (2001)

18 *Booy, M. L.:* Polym. Eng. Sci. 22, p. 433 (1982)

19 *Lee, C.-C.:* Polym. Eng. Sci. 30, p. 1607 (1990)

20 *Huneault, M. A., Lafleur, P. G., Carreau, P. J.:* Int. Polym. Process. 11, p. 50 (1996)

21 *Hurez, P., Tanguy, P. A.:* Polym. Eng. Sci. 33, p. 971 (1993)

22 *Vlachoploulos, J., Behncke, P., Vlcek, J.:* Adv. Polym. Tech 9, p. 147 (1989)

23 *Busby, J. W.:* Paper presented at the conference PVC '96, Brighton, England (1996)

24 *Gobeau, J. F., Coupez, T., Agassant, J. F., Vergnes, B.:* Paper presented at the 12th Annual Meeting of the Polymer Processing Society, Sorrento, Italy (1996)

25 *Schenkel, G., Kuhnle, H.:* Kunststoffe 73, p. 17 (1983)

26 *Kuhnle, H.:* Kunststoffe 76, p. 276 (1986)

27 *Carneiro, O. S., Nóbrega, J. M., Oliveira, P. J., Pinho, F. T.:* Int. Polym. Process. 18, p. 307 (2003)

28 *Nóbrega, J. M., Carneiro, O. S., Oliveira, P. J., Pinho, F. T.:* Int. Polym. Process. 18, p. 298 (2003)

29 *Carneiro, O. S., Nóbrega, J. M., Pinho, F. T., Oliveira, P. J.:* J. Mat. Process. Tech. 114, p. 75 (2001)

30 *Sienz, J., Marchal, J.-M., Pittman, J. F. T.:* Paper presented at the 3rd ESAFORM Conference, Stuttgart, Germany (2000)

31 *Reddy, M. P., Schaub, E. G., Reischneider, L. G., Thomas, H. L.:* Paper presented at the SPE Annual Technical Conference – ANTEC 99, New York, USA (1999)

32 *Langley, D. S., Pittman, J. F. T., Sienz, J.:* Paper presented at the 4th ESAFORM Conference, Liege, Belgium (2001)

33 *Oliveira, P. J., Pinho, F. T., Pinto, G. A.:* J. Non-Newt. Fluid Mech. 79, p. 1 (1998)

34 *Oliveira, P. J., Pinho, F. T.:* Num. Heat Transfer, Part B 35, p. 295 (1999)

35 *Nóbrega, J. M., Pinho, F. T., Oliveira., P. J., Carneiro, O. S.:* Int. J. Heat and Mass Transfer, in press

Date received: March 11, 2004
Date accepted: March 18, 2004

Acknowledgements

The authors gratefully acknowledge funding by FCT, Fundação para a Ciência e Tecnologia, under the POCTI and Pluriannual programmes.